to lower temperatures and will be completely suppressed by a field

$$H_{cr} \cong \frac{8K_1^{max}}{N_a M(0)} \cong 1 \text{ kOe},$$

where we take $M(0) = 7.55\mu_B$/atom.[5] Again this is in agreement with our measurements, although we do see a small critical field along the a axis which the theory does not explain.

It is clear from our measurements as well as others that the molecular-field model presented here is too simple to explain the detailed nature of this transition. Recently, Sherrington[19] has calculated the properties of an anisotropic ferromagnet at zero temperature in a more general way. In that model, as well, the change in sign of the lowest-order anisotropy constant leads to a second-order transition due, in that case, to the presence of a soft mode. We hope that the qualitative agreement between our experimental results and a molecular-field model will encourage a general treatment of the anisotropic ferromagnet at finite temperatures.

*Research supported in part by the Advanced Research Projects Agency under Contract No. HC15-67-C-0221.

†A. P. Sloan Research Fellow.

[1]W. D. Corner, W. C. Roe, and K. N. R. Taylor, Proc. Phys. Soc. (London) 80, 927 (1962).

[2]J. W. Cable and E. O. Wollan, Phys. Rev. 165, 733 (1968); also J. W. Cable (private communication).

[3]J. L. Féron and R. Pauthenet, Compt. Rend. 269, 549 (1969).

[4]K. P. Belov and A. V. Ped'ko, Zh. Eksperim. i Teor. Fiz. 42, 87 (1962) [Sov. Phys. JETP 15, 62 (1962)].

[5]H. E. Nigh, S. Legvold, and F. H. Spedding, Phys. Rev. 132, 1092 (1963).

[6]J. Alstad and S. Legvold, J. Appl. Phys. 35, 1752 (1964).

[7]R. M. Bozorth and T. Wakiyama, J. Phys. Soc. Japan 18, 97 (1963).

[8]M. Long, Jr., A. R. Wazzan, and V. R. Stern, Phys. Rev. 178, 775 (1969).

[9]F. Freyne, Phys. Rev. B 2, 1327 (1972).

[10]W. J. Nellis and S. Legvold, J. Appl. Phys. 40, 2267 (1969).

[11]T. Hiraoka and M. Suzuki, J. Phys. Soc. Japan 31, 1361 (1971).

[12]D. S. Simons and M. B. Salamon, Phys. Rev. Letters 26, 750 (1971).

[13]E. A. S. Lewis, Phys. Rev. B 1, 4368 (1970).

[14]M. E. Fisher and J. S. Langer, Phys. Rev. Letters 20, 665 (1968).

[15]R. D. Parks, in *Magnetism and Magnetic Materials*, edited by C. D. Graham, Jr. and J. J. Rhyne (A. I. P., New York, 1972), p. 630.

[16]H. B. Callen and E. Callen, J. Phys. Chem. Solids 27, 1271 (1966).

[17]L. D. Landau and E. M. Lifshitz, *Statistical Physics* (Pergamon, London, 1958), Chap. 14.

[18]M. Vicentini-Missoni, R. I. Joseph, M. S. Green, and J. M. H. Levelt-Sengers, Phys. Rev. B 1, 2312 (1970).

[19]D. Sherrington, Phys. Rev. Letters 28, 364 (1972).

PHYSICAL REVIEW B VOLUME 7, NUMBER 1 1 JANUARY 1973

Feynman-Graph Expansion for the Equation of State near the Critical Point*

E. Brézin† and D. J. Wallace‡
Joseph Henry Laboratories, Princeton University, Princeton, New Jersey 08540

and

Kenneth G. Wilson§
Institute for Advanced Study, Princeton, New Jersey 08540

(Received 14 July 1972)

The scaling equation of state for a generalized classical Heisenberg ferromagnet near the critical point is derived by an expansion in $\epsilon = 4 - d$, where d is the dimension of space. It is shown that, though infrared divergences are induced by the Goldstone modes, the equation of state is divergence free. The results are compared with previous numerical calculations. It is also shown that, for non-Ising-like systems the "linear model" cannot be exact, even at first order in ϵ (although the numerical deviations from linearity are small).

I. INTRODUCTION

The understanding of the physics of the critical region has been improved by the use of the ϵ expansion technique.[1,2] This method provides systematic corrections to mean-field theory by a perturbation expansion about four dimensions. Critical exponents have been calculated[2] and the known terms in the expansion in powers of $\epsilon = 4 - d$, where d is the dimension of space, give sensible results in three dimensions. In a previous work[3] the scaling equation of state was calculated up to order ϵ^2 for an Ising-like system. Here we present the details of a similar calculation, to the same order, for a generalized classical Heisenberg system.

The difference between this and the previous calculation is, first, that the weights of the various Feynman diagrams depend on n, the number of internal indices of the spin density. More important than this technical point is the fact that the responses of the system in directions parallel or transverse to the applied field are not the same. This is manifested by the appearance of massless Goldstone modes, i.e., the spin waves, below the critical temperature. These modes lead to new infrared divergences and it is shown that these divergences are absent from the equation of state, although they will appear in other physical quantities.

The results are compared with the numerical calculations[4,5] based on the extrapolation of high-temperature expansions.

The outline of the paper is as follows. Section II contains the notation and a description of the Hamiltonian. The perturbation expansion is outlined in Sec. III, with detailed calculations in Appendix A. In Sec. IV the equation of state is written in scaling form, and is compared both with previous numerical calculations and with a parametric form.

II. NOTATION; THE HAMILTONIAN

The spin density $s_i(x)$ has n internal degrees of freedom $i=1, 2, \ldots, n$. In the absence of any applied external field the Hamiltonian is symmetric under $O(n)$ transformations. By convention, the direction $i=n$ will be along the applied magnetic field H, and the Hamiltonian reads

$$\frac{\mathcal{H}}{kT}=\int d^dx\left[\frac{1}{2}\sum_{i=1}^{n}[(\nabla s_i)^2+r_0 s_i^2]+\frac{u_0}{4!}\left(\sum_1^n s_i^2\right)^2-Hs_n\right]. \tag{1}$$

It is convenient[6,7] to subtract from the longitudinal field $s_n(x)$ its expectation value, and to define a new field $L(x)$:

$$L(x)=s_n(x)-M\ , \tag{2}$$

$$M=\langle s_n(x)\rangle\ . \tag{3}$$

Then no "tadpole" insertions[7] of the field $L(x)$ are required.

Brackets denote the thermodynamic average which is defined as a functional integral

$$\langle A\rangle=\frac{\int \mathcal{D}s_i(x)\,e^{-\mathcal{H}/kT}A\{s_i(x)\}}{\int \mathcal{D}s_i(x)\,e^{-\mathcal{H}/kT}}\ , \tag{4}$$

and calculated by Feynman-graph expansion.

The Hamiltonian is then split into a free part

$$\frac{\mathcal{H}_0}{kT}=\frac{1}{2}\int d^dx\left(\sum_1^{n-1}(\nabla s_i)^2+(\nabla L)^2+r_T\sum_1^{n-1}s_i^2+r_L L^2\right) \tag{5}$$

and a perturbation

$$\frac{\mathcal{H}_1}{kT}=\int d^dx\left[\frac{u_0}{4!}\left(L^2+\sum_1^{n-1}s^2\right)^2+\frac{u_0}{3!}ML\left(L^2+\sum_1^{n-1}s_i^2\right)\right.$$
$$+\tfrac{1}{2}(r_0-r_L+\tfrac{1}{2}u_0M^2)L^2+\tfrac{1}{2}(r_0-r_T+\tfrac{1}{6}u_0M^2)$$
$$\left.\times\sum_1^{n-1}s_i^2+[(r_0+\tfrac{1}{6}u_0M^2)M-H]L\right]\ . \tag{6}$$

In contrast to Ref. 3, there are now two different renormalized "masses" r_L and r_T, corresponding to the fact that the longitudinal and transverse susceptibilities differ. Their precise definitions are given by

$$r_L^{-1}=\int d^dx\,[\langle s_n(x)s_n(0)\rangle-M^2]\ , \tag{7}$$

$$r_T^{-1}\delta_{ij}=\int d^dx\,\langle s_i(x)s_j(0)\rangle\ ,\quad 1\leq i,\ j\leq n-1\ . \tag{8}$$

As in previous works[2,3] the coupling constant u_0 is chosen in order to match the expected critical behavior of the renormalized quantities in zero field (above the critical temperature). The result is

$$u_0=\frac{48\pi^2}{n+8}\,\epsilon\left[1+\epsilon\left(\ln\Lambda+\frac{9n+42}{(n+8)^2}-\tfrac{1}{2}-\tfrac{1}{2}\ln 4\pi+\tfrac{1}{2}C\right)\right], \tag{9}$$

where Λ is a momentum cutoff much larger than the inverse of the longitudinal and transverse correlation lengths and C is Euler's constant. The cutoff is kept in intermediate steps but it will disappear from all physical quantities.

III. PERTURBATION THEORY

An expansion up to order ϵ^2 of the relation

$$\langle L(x)\rangle=0 \tag{10}$$

is performed. However, to be systematic, one must realize that the spontaneous magnetization is such that, although the u_0 vertex is of order ϵ, the u_0M vertex which appears in Eq. (6) is of order $\epsilon^{1/2}$. The three remaining vertices in $\mathcal{H}_1$ are merely counter terms which also vanish in zeroth order in ϵ. The one- and two-loop diagrams to be considered are shown in Figs. 1–3. Figure 1 shows the diagrams which contribute at order ϵ [and also ϵ^2 through the $(4-\epsilon)$-dimensional integrations]. The diagrams of Fig. 3 contain a propagator insertion; the mass counter terms are taken into account by subtracting the insertion at zero momentum. The evaluation of these diagrams is given in Appendix A.

The bare quantity r_0 is a linear measure of the temperature, and it is eliminated in favor of the reduced temperature $t=(T-T_c)/T_c$, by subtracting from the relation $\langle L(x)/M\rangle=0$, its expression at the critical point $T=T_c$, $H=M=0$. This yields a relation between H, t, M, r_L, and r_T which reads

$$\frac{H}{M}=t+\tfrac{1}{6}u_0M^2+\frac{\epsilon}{2(n+8)}\left[1+\epsilon\left(\frac{9n+42}{(n+8)^2}+\ln\Lambda\right)\right]+\left[3r_L(\ln r_L-2\ln\Lambda-\tfrac{1}{4}\epsilon\ln^2 r_L)+(n-1)r_T(\ln r_T-2\ln\Lambda-\tfrac{1}{4}\epsilon\ln^2 r_T)\right]$$
$$-\frac{\epsilon^2}{2(n+8)^2}\left[(n+8)r_L(\ln r_L+2\ln\Lambda\ln r_L-\tfrac{1}{2}\ln^2 r_L)+2(n-1)r_T(\ln r_T+2\ln\Lambda\ln r_T-\tfrac{1}{2}\ln^2 r_T)+(n-1)r_L I_1(\rho)\right]$$
$$+\frac{9u_0M^2\epsilon^2}{(n+8)^2}\Bigg[\tfrac{1}{4}[2\ln r_L(\ln\Lambda-1)-\tfrac{1}{2}\ln^2 r_L]+\frac{n-1}{36}[\tfrac{1}{2}\ln^2 r_L-\ln r_L\ln r_T-\ln r_L-(1-2\ln\Lambda)\ln r_T-I_1(\rho)-I_2(\rho)]$$
$$+\frac{n-1}{54}\left(-\tfrac{1}{2}\ln^2 r_L+(2\ln\Lambda-1)\frac{r_L\ln r_L-r_T\ln r_T}{r_L-r_T}+\frac{r_T\ln r_T\ln r_L/r_T}{r_L-r_T}+I_3(\rho)\right)\Bigg]\ , \qquad (11)$$

where $\rho=r_L/4r_T$ and the functions I_1, I_2, I_3 are defined in Appendix A.

In order to get the equation of state the quantities r_L and r_T have to be expressed in terms of the basic variables H, M, and t. This may be done by a diagrammatic expansion of the expressions (7) and (8) which define them. However, it is much simpler to use the relations

$$r_L=\left(\frac{\partial H}{\partial M}\right)_t \qquad (12)$$

and

$$r_T=H/M\ , \qquad (13)$$

the first of which follows from the definitions (3) and (7) of M and r_L. The second relation follows simply if one takes for granted a relation of the form

$$\vec{\mathrm{H}}=\vec{\mathrm{M}}\,F(M^2,t)\ ,$$

and is also pedantically derived as a Ward identity in Appendix B.

Equations (11)–(13) provide an implicit definition of the equation of state. From the Ward identity (13) the existence of the massless Goldstone modes is manifest: r_T vanishes with H below T_c since M remains finite. This leads to an apparent infrared divergence of the expression (11) for H/M at the coexistence curve ($H=0$, $t<0$). However, a similar divergence also appears in r_L as can be seen from Eqs. (11) and (12), or directly from the fact that a closed loop of the transverse modes contributes to the longitudinal propagator,[8] as shown in Fig. 4. The equation of state must not exhibit these divergences in order to be meaningful in the vicinity of the coexistence curve. And indeed, when r_L is eliminated between Eqs. (11) and (12), the diverging $\ln r_T$ terms do cancel.

IV. EQUATION OF STATE IN SCALING FORM

Describing the coexistence curve as $-t\propto M^{1/\beta}$, and the critical isotherm as $H\propto M^\delta$, one obtains, from Eq. (11),

$$\frac{1}{\beta}=2+\frac{6}{n+8}\epsilon+4\frac{(n+5)(7-n)}{(n+8)^3}\epsilon^2+O(\epsilon^3)\ , \qquad (14)$$

$$\delta=3+\epsilon+\frac{n^2+14n+60}{2(n+8)^2}\epsilon^2+O(\epsilon^3)\ . \qquad (15)$$

Then the scaling equation of state is obtained as a relation between $y=H/M^\delta$ and $x=t/M^{1/\beta}$. The result does not appear naturally in the simple Griffiths[9] form $y=f(x)$, but rather as an implicit relation,

$$y=x+\tfrac{1}{6}u+\frac{\epsilon}{2(n+8)}\left[3(x+\tfrac{1}{2}u)\ln(x+\tfrac{1}{2}u)+(n-1)y\ln y+\tfrac{1}{3}(n+8)u\left(\frac{9n+42}{(n+8)^2}-\tfrac{1}{2}-\tfrac{1}{2}\ln 4\pi+\tfrac{1}{2}C\right)\right]$$
$$+\epsilon^2\Bigg\{\frac{3(x+\frac{1}{2}u)(10-n)+u(26+n)}{24(n+8)^2}\ln^2(x+\tfrac{1}{2}u)+\frac{(n-1)y\ln y\ln(x+\frac{1}{2}u)}{4(n+8)^2}-\frac{n(n-1)y\ln^2 y}{8(n+8)^2}$$
$$+\left[\frac{212+17n-4n^2}{4(n+8)^3}(x+\tfrac{1}{2}u)+\frac{3u}{4(n+8)}\left(\frac{9n+42}{(n+8)^2}-\tfrac{1}{2}+\tfrac{1}{2}C-\tfrac{1}{2}(\ln 4\pi)\right)\right]\ln(x+\tfrac{1}{2}u)$$
$$+\frac{(n-1)(19n+92)}{4(n+8)^3}y\ln y-\frac{(n-1)}{2(n+8)^2}(x+\tfrac{1}{2}u)I_1(\rho)-\frac{u(n-1)}{4(n+8)^2}[I_1(\rho)+I_2(\rho)]+\frac{u(n-1)}{6(n+8)^2}I_3(\rho)\Bigg\}\ , \qquad (16)$$

where

$$u\equiv[48\pi^2/(n+8)]\,\epsilon\ .$$

It is possible to solve Eq. (16) for y in powers of ϵ. If the fields and temperature scales are set by

$$H/M^\delta=1 \quad \text{at } t=0$$

and

$$-t/M^{1/\beta}=1 \quad \text{at } H=0\ ,\quad t<0 \qquad (17)$$

the solution reads $y=f(x)$ with

$$
\begin{aligned}
f(x)=x+1+\frac{\epsilon}{2(n+8)}&\left(1+\frac{\epsilon}{2(n+8)}[n-1+6\ln 2-9\ln 3+(n-1)\ln(x+1)]\right)\\
&\times[3(x+3)\ln(x+3)+(n-1)(x+1)\ln(x+1)+6x\ln 2-9(x+1)\ln 3]+\left(\frac{\epsilon}{2(n+8)}\right)^2\\
&\times\Big(\tfrac{1}{2}(10-n)(x+1)[\ln^2(x+3)-\ln^2 3]+36[\ln^2(x+3)-(x+1)\ln^2 3+x\ln^2 2]-54\ln 2[\ln(x+3)+x\ln 2-(x+1)\ln 3]\\
&\quad+3(n-1)\left(\ln\tfrac{27}{4}\right)(x+1)\ln(x+1)+\frac{212+17n-4n^2}{n+8}[(x+3)\ln(x+3)+2x\ln 2-3(x+1)\ln 3]\\
&\quad+(n-1)(x+1)\ln(x+1)\ln(x+3)-\tfrac{1}{2}n(n-1)(x+1)\ln^2(x+1)+\frac{n-1}{n+8}(19n+92)(x+1)\ln(x+1)\\
&\quad-2(n-1)\left[(x+6)I_1(\rho)-6(x+1)I_1(\tfrac{3}{4})\right]-6(n-1)\left[I_2(\rho)-(x+1)I_2(\tfrac{3}{4})\right]+4(n-1)\left[I_3(\rho)-(x+1)I_3(\tfrac{3}{4})\right]\Big)\ ,
\end{aligned}
\tag{18}
$$

where

$$\rho=(x+3)/4(x+1)\ .$$

As it stands the expression (18) for $f(x)$ suffers from two defects. (i) The process of solving for y has violated the positivity of y, which was satisfied by the original Eq. (16), but only in the extremely small range

$$0\leq x+1\lesssim\exp\left(-\frac{(n+8)}{2(n-1)\epsilon}\right)\ .$$

(ii) More seriously, Griffiths's conditions on the large-x behavior[9] of $f(x)$, namely,

$$f(x)=\sum_{n=1}^{\infty}a_n x^{\gamma-2(n-1)\beta}\ ,\quad x\to\infty \tag{19}$$

are only satisfied within the framework of the ϵ expansion, but not explicitly. For example, the leading terms of $f(x)$, for large x, are

$$
\begin{aligned}
f(x)\sim\left(1+\frac{3\epsilon}{2(n+8)}\ln\tfrac{4}{27}\right)&\left[x+\frac{\epsilon(n+2)}{2(n+8)}x\ln x\right.\\
&\left.+\epsilon^2\left(\frac{(n+2)^2}{8(n+8)^2}x\ln^2 x+\frac{(n+2)(n^2+22n+52)}{4(n+8)^2}x\ln x\right)\right]\ ,\\
&\qquad x\to\infty
\end{aligned}
\tag{20}
$$

which is indeed proportional to the ϵ expansion of x^{γ} with the value obtained in Ref. 2:

$$\gamma=1+\frac{n+2}{2(n+8)}\epsilon+\frac{(n+2)(n^2+22n+52)}{4(n+8)^3}\epsilon^2+O(\epsilon^3)\ . \tag{21}$$

Nevertheless, with no attempt to remedy these defects by replacing f with a more satisfactory expression equivalent at order ϵ^2, the orders zero, one, and two in ϵ have been compared with the numerical calculations of Gaunt and Domb on the three-dimensional Ising model[4] ($n=1$), and with the Milošević and Stanley results for the Heisenberg model[5] ($n=3$). The comparison is displayed in Figs. 5 and 6. Though the successive corrections to the zeroth order do go in the right direction, the agreement with the high-temperature extrapolations is better[10] for $n=1$. This is not surprising since the large-x behavior of $f(x)$ is governed mainly by the value of γ, and in Ref. 5 the value of γ is determined as 1.43, whereas the ϵ series gives $\gamma=1.34$ for $n=3$. This simple fact accounts for approximately 75% of the discrepancy for $x=5$. Therefore, the relevance of the comparison lies mainly in showing that the ϵ and ϵ^2 terms in Eq. (18) provide meaningful corrections.

V. PARAMETRIC FORMS

It is well known that the best way of obtaining an equation of state consistent with Griffiths's conditions (19) is to write it in parametric form,[11,12] i.e., H, M, and t are expressed as

$$
\begin{aligned}
&H=R^{\beta\delta}h(\theta)\ ,\\
&M=R^{\beta}m(\theta)\ ,\\
&t=R\tau(\theta)\ ,
\end{aligned}
\tag{22}
$$

where all the nonanalyticity is contained in the R dependence. In order to compare with the "linear model,"[12] we make the choice

$$
\begin{aligned}
&h(\theta)=a\theta(1-\theta^2)\ ,\\
&\tau(\theta)=1-b^2\theta^2\ ,
\end{aligned}
\tag{23}
$$

solve for $m(\theta)$, and explore to what extent it is linear in θ. Each parameter in Eqs. (23) has to be expanded in powers of ϵ. Working for simplicity to order ϵ, we write

$$
\begin{aligned}
&a=a_0(1+\epsilon a_1)\ ,\quad b^2=b_0^2(1+\epsilon b_1)\ ,\\
&m(\theta)=c_0\theta[1+\epsilon m_1(\theta)]\ .
\end{aligned}
\tag{24}
$$

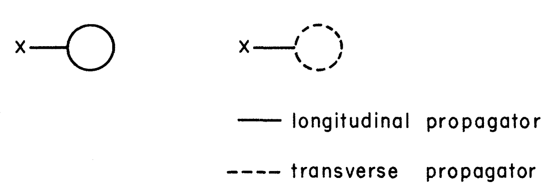

FIG. 1. First-order contributions to Eq. (10).

FIG. 2. Second-order contributions to Eq. (10).

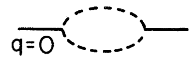

$$\propto \int \frac{d^4 q}{(q^2+r_T)^2} \propto \ln r_T$$

FIG. 4. Source of the infrared divergence of the longitudinal susceptibility.

The equation of state is satisfied at this order with

$$\begin{aligned} &a_0 = c_0 , \quad b_0^2 = a_0^2 + 1 , \\ &m_1(\theta) = a_1(1-\theta^2) + \tfrac{3}{2} b_1 \theta^2 - [1/2(n+8)] \\ &\qquad \times \{ (n-1)(1-\theta^2)\ln(1-\theta^2) \\ &\qquad + 3[1+(2b_0^2-3)\theta^2]\ln[1+(2b_0^2-3)\theta^2] \\ &\qquad\quad + 6(1-b_0^2\theta^2)\ln 2 - 9(1-\theta^2)\ln 3\} . \end{aligned} \tag{25}$$

Additional criteria are required in order to decide which set of parameters should be chosen. Nevertheless, when n is greater than 1, there is no choice for which $m_1(\theta)$ is a constant [or $m(\theta)$ linear], although the linear model can be numerically satisfactory. For example, the choice

$$b_0^2 = \tfrac{3}{2} , \quad m_1(0) = m_1(1)$$

leads to

$$m_1(\theta) = \text{const}\left(1 - \frac{\epsilon(n-1)}{2(n+8)}(1-\theta^2)\ln(1-\theta^2)\right) .$$

When $n = 3$, and in three dimensions, this differs from a constant by at most 3%.

VI. CONCLUSION

It is clear that the ϵ expansion provides meaningful corrections to mean-field theory both for critical exponents and for the scaling equation of state. It also provides some quantitative understanding of the validity and limitations of phenomenological descriptions such as the linear model.

However, one problem remains. The equation of state is indeed finite at the coexistence curve, but thermodynamic quantities involving derivatives of the magnetic field, such as the magnetic susceptibility and the specific heat at constant magnetization, are infrared divergent below T_c, when H goes to zero.[13] In perturbation theory these divergences appear as powers of $\epsilon \ln r_T$. It is clear that such terms arise from the ϵ expansion of r_T raised to some power depending on ϵ. The precise behavior of the system near the coexistence curve requires the knowledge of the form to which these terms should be exponentiated.

On the basis of an argument relying on the freedom of making nonlinear realizations[14] of the $O(n)$ symmetry, it is conjectured that

$$r_L^{-1} \sim \text{const} + r_T^{-\epsilon/2} , \quad H \to 0 , \quad T < T_c$$

for all $n > 1$ and to all orders in ϵ.

The ability of the Feynman-graph method to reproduce such a result requires further study since, in principle, additional transient terms in the recursion formulas might appear in this region (where two length scales exist). An exact treatment involves a study of the renormalization group equations[15] below T_c.

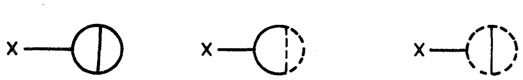

FIG. 3. Propagator insertions contributing to Eq. (10).

APPENDIX A: EVALUATION OF FEYNMAN DIAGRAMS

As explained in the text all diagrams must be subtracted at the critical point where M, r_L, and r_T vanish.

(i) Diagrams of Fig. 1 are to be evaluated up to order ϵ^2 retaining only at that order the relevant $\ln r$ behavior. This requires the evaluation of

$$\begin{aligned} &\frac{1}{(2\pi)^d}\int_{q^2<\Lambda^2} d^d q \left(\frac{1}{q^2+r} - \frac{1}{q^2}\right) \\ &= \frac{2\pi^2}{(2\pi)^4}[1 + \tfrac{1}{2}\epsilon(\ln 4\pi + 1 - C)] \\ &\quad \times \int_0^\Lambda dq\, q^3(1-\epsilon\ln q)\left(\frac{1}{q^3+r} - \frac{1}{q^2}\right) + O(\epsilon^2) \\ &\sim \frac{1}{16\pi^2}[1+\tfrac{1}{2}\epsilon(\ln 4\pi + 1 - C)]\, r[\ln r/\Lambda^2 - \tfrac{1}{4}\epsilon \ln^2 r] , \end{aligned}$$

where C is Euler's constant.

(ii) The first diagram of Fig. 2 involves only r_L:

$$\begin{aligned} &\int \frac{d^4 q_1\, d^4 q_2}{(2\pi)^8} \{ [(q_1^2 + r_L)(q_2^2 + r_L)((\vec{q}_1 + \vec{q}_2)^2 + r_L)]^{-1} \\ &\qquad - [q_1^2 q_2^2 (\vec{q}_1 + \vec{q}_2)^2]^{-1} \} \\ &\sim \frac{3}{256\pi^4}\, r[(1+2\ln\Lambda)\ln r - \tfrac{1}{2}\ln^2 r] . \end{aligned}$$

The second diagram of Fig. 2, having two different masses r_L and r_T in the propagators, produces a nonelementary function of the ratio

$$\rho = r_L / 4 r_T .$$

Through the use of Feynman parameters, we obtain

$$\begin{aligned} &\int \frac{d^4 q_1\, d^4 q_2}{(2\pi)^8} \{ [(q_1^2 + r_T)(q_2^2 + r_T)((\vec{q}_1 + \vec{q}_2)^2 + r_L)]^{-1} \\ &\qquad - [q_1^2 q_2^2 (\vec{q}_1 + \vec{q}_2)^2]^{-1} \} \end{aligned}$$

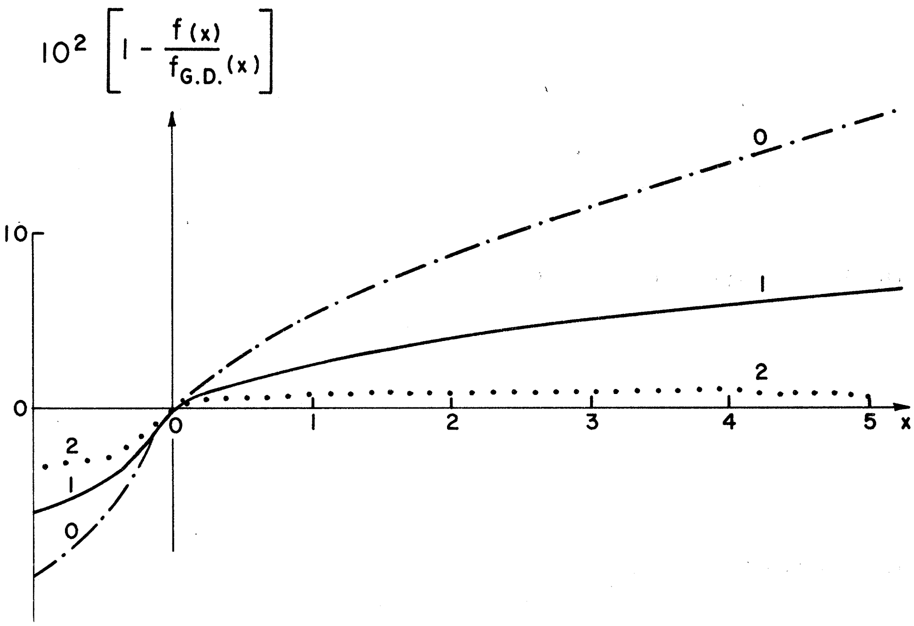

FIG. 5. Comparison with the results of Gaunt and Domb on the Ising model at order 0, 1, and 2 in ϵ.

$$\sim \frac{1}{256\pi^4}\left[(1+2\ln\Lambda) r_L \ln r_L - (\tfrac{1}{2} r_L)\ln^2 r_L + 2(1+2\ln\Lambda) r_T \ln r_T - r_T \ln^2 r_T + r_L I_1(\rho)\right],$$

where the function $I_1(\rho)$ may be written

$$I_1(\rho)=\int_0^\rho \frac{du \ln u}{u(1-u)}\left[(1-u/\rho)^{1/2}-1\right]-\int_\rho^\infty \frac{du\ln u}{u(1-u)} .$$

When ρ tends to infinity (coexistence curve),

$$I_1(\rho)\sim (1/4\rho)(\ln^2 4\rho + 2\ln\rho)+O(1/\rho), \quad \rho\to\infty .$$

(iii) Similarly, the first diagram of Fig. 3 involves only r_L and gives simply

$$\int \frac{d^4q_1\, d^4q_2}{(2\pi)^8}\,\frac{1}{(q_1^2+r_L)^2}\left\{\left[(q_2^2+r_L)\left((\vec{q}_1+\vec{q}_2)^2+r_L\right)\right]^{-1} - (q_2^2+r_L)^{-2}\right\} \sim \frac{1}{256\pi^4}\left[-\tfrac{1}{2}\ln^2 r_L + 2(\ln\Lambda-1)\ln r_L\right] .$$

The last two diagrams of Fig. 3 also depend on ρ in a nonelementary way. The first one is

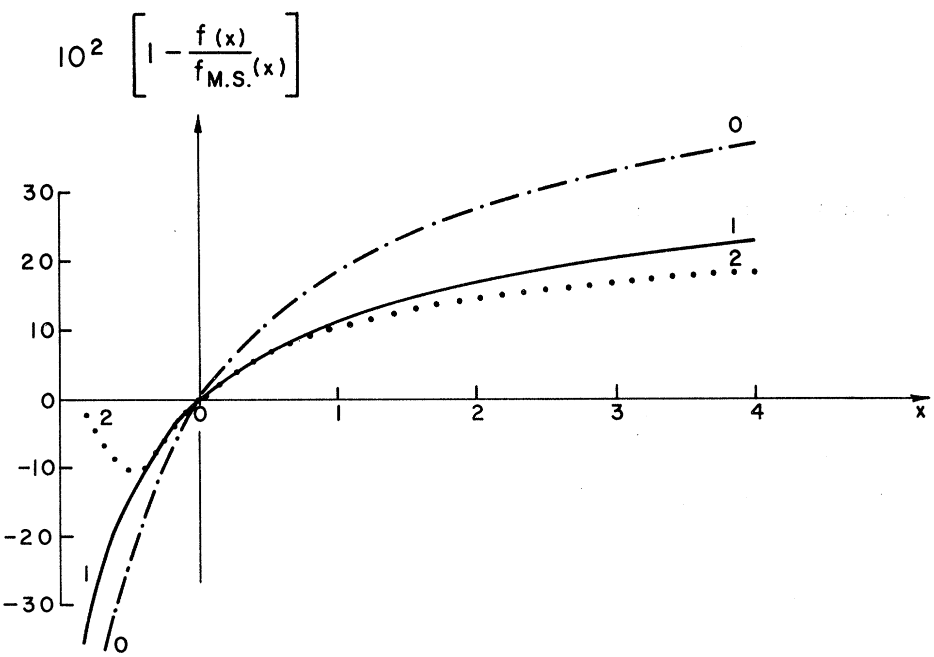

FIG. 6. Comparison with the results of Milošević and Stanley on the Heisenberg model at order 0, 1, and 2 in ϵ.

$$\int \frac{d^4q_1\,d^4q_2}{(2\pi)^8}\,\frac{1}{(q_1^2+r_L)^2}\,\{[(q_2^2+r_T)((\vec{q}_1+\vec{q}_2)^2+r_T)]^{-1} - (q_2^2+r_T)^{-2}\}$$

$$\sim \frac{1}{256\pi^4}\,[\tfrac{1}{2}\ln^2 r_L - \ln r_L - \ln r_L \ln r_T + (2\ln\Lambda - 1)\ln r_T - I_1(\rho) - I_2(\rho)]\ ,$$

where

$$I_2(\rho) = \frac{1}{2\rho}\int_0^\rho \frac{du \ln u}{1-u}\left(1-\frac{u}{\rho}\right)^{-1/2}\ .$$

Near the coexistence curve, the asymptotic behavior of I_2 is

$$I_2(\rho) \sim -(1/4\rho)\ln^2 4\rho + O(1/\rho)\ ,\quad \rho\to\infty\ .$$

The last diagram gives, similarly,

$$\int \frac{d^4q_1\,d^4q_2}{(2\pi)^8}\,\frac{1}{(q_1^2+r_T)^2}\,\{(q_2^2+r_T)^{-1}[(\vec{q}_1+\vec{q}_2)^2+r_L]^{-1} - (q_2^2+r_T)^{-1}(q_2^2+r_L)^{-1}\}$$

$$\sim \frac{1}{256\pi^4}\left(-\tfrac{1}{2}\ln^2 r_L + \frac{1}{r_L-r_T}\,[(2\ln\Lambda - 1)(r_L \ln r_L - r_T\ln r_T) + r_T \ln r_T \ln r_L/r_T] + I_3(\rho)\right)\ ,$$

where

$$I_3(\rho) = \int_0^\rho \frac{du\ln u}{u(1-u)}[(1-u/\rho)^{-1/2}-1] - \int_\rho^\infty \frac{du \ln u}{u(1-u)}\ .$$

For ρ large,

$$I_3(\rho) \sim \frac{1}{4\rho}\,(-\ln^2 4\rho + 2\ln\rho) + O\left(\frac{1}{\rho}\right)\ ,\quad \rho\to\infty\ .$$

As a final remark, we note the following relations:

$$I_1(\rho) + 2I_2(\rho) = I_3(\rho)\ ,\quad I_2(\rho) = \rho\,\frac{dI_1}{d\rho}\ .$$

APPENDIX B: BROKEN $O(n)$ SYMMETRY AND WARD IDENTITIES

The generating functional[16] for connected Green's functions is defined as the Feynman integral

$$e^{-F(H_i)} = \int \mathfrak{D}s_i(x)\,e^{-\mathcal{H}/kT}\ ,$$

where $\mathcal{H}/kT$, in addition to an $O(n)$ invariant part, contains an external source term

$$\sum_{i=1}^n \int H_i(x)\,s_i(x)\,d^dx\ .$$

Apart from the source term the integral is invariant under the substitutions

$$s_i(x) \to s_i(x) + \omega^\alpha\, c_{ij}^\alpha\, s_j\ ,$$

where ω^α is an infinitesimal rotation about the α axis and c_{ij}^α is antisymmetric in i and j. The variation of the source term under this transformation leads to the relation

$$F(H_i) = F(H_i - \omega^\alpha c_{ij}^\alpha H_j)\ ,$$

or in differential form, to

$$\sum_{ij}\int \frac{\delta F}{\delta H_i(x)}\,H_j(y)\,c_{ji}^\alpha = 0\ .$$

We choose now $H_n(x)$ as the constant longitudinal field H, differentiate with respect to a transverse component $H_k(y)$ $(k<n)$, and set all transverse components to zero. This yields

$$\frac{\delta F}{\delta H_L}\,c_{kn}^\alpha + \int d^dx\,\frac{\delta^2 F}{\delta H_i(x)\delta H_k(y)}\bigg|_{H_T=0} H_L\, c_{ni}^\alpha = 0\ ,$$

which, though the definitions of M and r_T and the antisymmetry of c^α, simplifies to

$$r_T = H/M\ .$$

---

*Research sponsored by the U. S. Atomic Energy Commission, under Contract No. AT(11-1)-3072.

†On leave from Service de Physique Théorique, Saclay, B. P. No. 2, 91 Gif-sur-Yvette, France.

‡Harkness Fellow. Permanent address: University of Southampton, England.

§On leave from Cornell University, Ithaca, N. Y. 14850.

[1]K. G. Wilson and M. E. Fisher, Phys. Rev. Letters 28, 240 (1972).

[2]K. G. Wilson, Phys. Rev. Letters 28, 548 (1972).

[3]E. Brézin, D. J. Wallace, and K. G. Wilson, Phys. Rev. Letters 29, 591 (1972).

[4]D. S. Gaunt and C. Domb, J. Phys. C 3, 1442 (1970).

[5]S. Milošević and H. E. Stanley, Phys. Rev. B 5, 2526 (1972).

[6]This Hamiltonian has the same form (when $n=4$) as the Gell-Mann and Lévy σ model of strong-interaction pion dynamics, and many of the features of the following calculations have been previously discussed in this latter framework. M. Gell-Mann and M. Lévy, Nuovo Cimento 16, 705 (1960).

[7]The perturbation theory and the renormalizability of the linear σ model have been discussed by B. W. Lee, Nucl. Phys. B9, 649 (1969).

[8]The same divergences have been noted for the σ model by D. Bessis and J. Zinn-Justin, Phys. Rev. D 5, 1313 (1972).

[9]R. B. Griffiths, Phys. Rev. 158, 176 (1967).

[10]The graph for $n=1$ differs from the graph shown in Ref. 3 because there $f(x)$ was normalized by

$$f(x) = \frac{x+1+\epsilon f_1(x)+\epsilon^2 f_2(x)}{1+\epsilon f_1(0)+\epsilon^2 f_2(0)}\ ,$$

whereas here the denominator is explicitly expanded to order ϵ^2.

[11]B. D. Josephson, J. Phys. C 2, 1113 (1969).

[12]P. Schofield, J. D. Litster, and J. T. Ho, Phys. Rev. Letters 23, 1098 (1969), and the references therein.

[13]This possibility is discussed by M. E. Fisher, Rept.

Progr. Phys. 30, 645 (1967).

[14]It is easy to show that the logarithmic divergences cancel in the specific heat at constant field. This suggests that the energy fluctuations remain finite on the coexistence curve, and invites the exploration of nonlinear realizations in which $\sum_1^n s_i^2$ is kept constant, as suggested in Ref. 6 and studied extensively by S. Weinberg, Phys. Rev. 166, 1568 (1968).

[15]A review of the use of the renormalization group equation in this framework is given by K. G. Wilson and J. B. Kogut, Phys. Rept. (to be published).

[16]We have followed the standard method as, for example, in B. W. Lee, *Chiral Dynamics* (Gordon and Breach, New York, to be published).

PHYSICAL REVIEW B VOLUME 7, NUMBER 1 1 JANUARY 1973

Surface States of an Induced-Moment System and a Hydrogen-Bonded Ferroelectric*

D. A. Pink

Department of Physics, St. Francis Xavier University, Antigonish, Nova Scotia, Canada

(Received 20 July 1972)

We have investigated the surface bound states and resonances that occur on a (001) surface of either a two-level induced-moment system or the tunneling model of a hydrogen-bonded ferroelectric. We have assumed (a) that there is a perfectly sharp surface and (b) that only parameters on the surface have values different from those in the bulk of the crystal, and we have used the random-phase approximation to solve the equations of motion for the thermodynamic Green's functions. Analytical expressions have been obtained for the complete Green's functions. Three phases can exist: (i) Both the surface and the bulk are disordered, (ii) the surface is ordered but the bulk is disordered, or (iii) both the surface and the bulk are ordered. In phases (i) and (ii) only one kind of localized mode can appear, while in phase (iii) two kinds, localized on the first and second layers, can exist. No resonances appear inside the bulk band when both surface and bulk are disordered, but resonances can appear in the other two phases. Some criteria for the appearance of bound states have been derived and numerical calculations have been carried out for the three phases at zero temperature. Some experiments are suggested.

I. INTRODUCTION

There has been considerable interest recently in the modes that are localized on and near the surface of magnetically ordered crystals which are described by the Heisenberg Hamiltonian with possibly anisotropic exchange interactions. We shall be concerned here with modes that occur upon one surface of an otherwise infinite or periodic crystal. Early work was done by Wallis *et al.*[1] and Mills and Maraduddin[2] on the Heisenberg ferromagnet and was concerned with the modes excited on a free surface (whereon the exchange interaction is the same as that in the bulk) and their effects on thermodynamic quantities. Other early works were those of Fillipov[3] (see also deWames and Wolfram[4]) and Mills,[5] who investigated the effect of changing the exchange interactions upon the surface and between the surface and second layer from that of the bulk. This problem was also treated by deWames and Wolfram[6] (see also Ilisca and Motchane[7]). These authors restricted themselves to isotropic interactions. More recently, the effects of exchange anisotropy has been considered by Osborne,[8] Ilisca and Motchane,[7] and Levy, Ilisca, and Motchane,[9] together with next-nearest-neighbor exchange coupling by Levy, Ilisca, and Motchane.[10] Recent work on the Heisenberg antiferromagnet has been done by Mills[11] on the surface spin-flop state and by Mills and Saslow[12] on surface effects in general, while Sparks[13] has considered both the ferro- and antiferromagnet.

There is, however, a large class of magnetically ordered systems for which the Hamiltonian may contain, in addition to the bilinear Heisenberg term, terms due to the effects of crystal fields. The magnetic behavior of such systems is of particular interest when the magnitude of the crystal field parameters is comparable to that of the exchange interaction, which is the situation that appears to exist in the light rare-earth metals. One of the best-studied examples is that of Pr^{3+} ions in various crystal field environments (see Rainford and Gylden Houmann[14] and other references therein). In a hexagonal crystal field, the lowest ionic states are a magnetic singlet, a higher-lying singlet, and a doublet. Because the z component of the total magnetic-moment operator $\vec{J}$ has a nonzero matrix element between the two singlets, a nonzero value of magnetization can occur if the ratio of the magnitude of the exchange interaction to that of the crystal field splitting between the two singlets is sufficiently large. Here we shall assume that the system with which we are concerned has two nondegenerate singlets as the